Superconducting–magnetic heterostructures: a method of decreasing AC losses and improving critical current density in multifilamentary conductors

2009 J. Phys.: Condens. Matter 21 254206

(http://iopscience.iop.org/0953-8984/21/25/254206)

J. Phys.: Condens. Matter **21** (2009) 254206 (10pp) doi:10.1088/0953-8984/21/25/254206

Superconducting–magnetic heterostructures: a method of decreasing AC losses and improving critical current density in multifilamentary conductors

B A Glowacki[1] **and M Majoros**[2]

[1] Department of Materials Science and Metallurgy, University of Cambridge, Pembroke Street, Cambridge CB2 3QZ, UK
[2] College of Engineering, The Ohio State University, 555 MacQuigg Laboratory, 105 W Woodruff Avenue, Columbus, OH 43210, USA

E-mail: bag10@cam.ac.uk (B A Glowacki)

Received 31 March 2009
Published 29 May 2009
Online at stacks.iop.org/JPhysCM/21/254206

Abstract
Magnetic materials can help to improve the performance of practical superconductors on the macroscale/microscale as magnetic diverters and also on the nanoscale as effective pinning centres. It has been established by numerical modelling that magnetic shielding of the filaments reduces AC losses in self-field conditions due to decoupling of the filaments and, at the same time, it increases the critical current of the composite. This effect is especially beneficial for coated conductors, in which the anisotropic properties of the superconductor are amplified by the conductor architecture. However, ferromagnetic coatings are often chemically incompatible with $YBa_2Cu_3O_7$ and $(Pb, Bi)_2Sr_2Ca_2Cu_3O_9$ conductors, and buffer layers have to be used. In contrast, in MgB_2 conductors an iron matrix may remain in direct contact with the superconducting core. The application of superconducting–magnetic heterostructures requires consideration of the thermal and electromagnetic stability of the superconducting materials used. On one hand, magnetic materials reduce the critical current gradient across the individual filaments but, on the other hand, they often reduce the thermal conductivity between the superconducting core and the cryogen, which may cause destruction of the conductor in the event of thermal instability. A possible nanoscale method of improving the critical current density of superconducting conductors is the introduction of sub-micron magnetic pinning centres. However, the volumetric density and chemical compatibility of magnetic inclusions has to be controlled to avoid suppression of the superconducting properties.

(Some figures in this article are in colour only in the electronic version)

1. Introduction

Magnetic materials can help to improve the performance of practical superconductors on the macro/microscale as magnetic diverters and also on the nanoscale as effective pinning centres.

It is well documented that ferromagnetic materials acting as magnetic flux diverters and screens can effectively reduce the exposure of the superconducting material to an external magnetic field and therefore improve the in-field performance of practical superconductors [1]. The external magnetic field may originate from neighbouring elements or electromagnets, as in the case of current leads or from neighbouring strands and phases in superconducting cables [2–4]. A strong influence of the presence of ferromagnetic substrates, coatings and buffer layers on the magnetic flux distribution from neighbouring filaments has also been calculated for practical multifilamentary $YBa_2Cu_3O_7$, $(Pb, Bi)_2Sr_2Ca_2Cu_3O_9$ and MgB_2 conductors [5, 6]. The prospect of using low-cost, highly-textured Ni-based substrates [7, 8] has stimulated

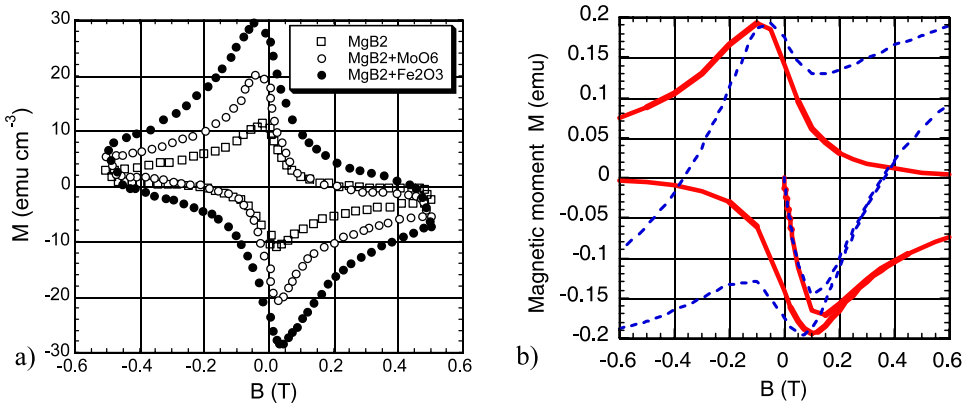

Figure 1. Magnetization of MgB_2 nanocomposites: (a) comparison of MgB_2 with high-intensity ultrasound treated $MgB_2 + Mo_2O_6$ and $MgB_2 + Fe_2O_3$, after [11, 15]; (b) comparison of MgB_2 (solid line) with an unannealed mixture of $MgB_2 + Fe$ in a (Cu/MgB_2 + 10% Fe) conductor (dotted line), magnetic field applied along the wire axis.

research concerning potential architectures of superconducting cables in which ferromagnetic substrates can be used [2, 9]. These calculations are very valuable, but because they are just 2D models they do not take into account the real helical configuration of the tapes in the cable [10–13]: the transversal distribution of the current in the conductor increases the participation of the ferromagnetic substrate material in the overall losses of the cable.

Improvement of the transport properties of conductors by the addition of nanoscale/sub-micron magnetic pinning centres has recently been considered more widely, driven by progress in understanding superconducting/ferromagnetic interfaces [14–17]. However, the volumetric density and chemical compatibility of magnetic nano-inclusions has to be controlled [18] to avoid suppression of the superconducting properties over distances larger than the coherence length [15].

In this paper we will discuss aspects of the influence of ferromagnetic materials on the properties of practical $YBa_2Cu_3O_7$, $(Pb, Bi)_2Sr_2Ca_2Cu_3O_9$ and MgB_2 multifilamentary conductors.

2. Ferromagnetic pinning centres

Important aspects of the coexistence of superconducting and ferromagnetic materials include interfacial reaction, especially in the case of MgB_2 and the magnetic properties of ferromagnetic particles at low temperatures from 4.2 to 77 K. There is an open question if magnetic pinning centres should be made from iron or from iron oxides. It was shown by Grovenor [18] that the MgB_2/Fe interface shows some detectable chemical interaction, causing formation of Fe–B compounds.

For very small ferromagnetic (FM) particles the magnetic anisotropy energy K_a is comparable to the thermal energy, kT. When this happens, the particles become superparamagnetic; thermal fluctuations randomly flip the magnetization direction between the parallel and antiparallel orientations. This differs from conventional paramagnetism because the effective moment of the particle is the sum of its ionic particles, which can be several thousand spins in a ferromagnetic particle small enough to show superparamagnetism. In our experiments, iron powder was added to MgB_2 powder, which was then mixed, ground and annealed. It was evident that the higher concentration of Fe in MgB_2 dominates the behaviour of the Cu/(MgB_2 + Fe) composite irrespective of the sintering procedure.

Prozorov *et al* [15, 19] observed that the magnetic pinning force is a long-range attractive force with a characteristic length λ. The magnitude of this force depends on the magnetization value, particle size and orientation of the magnetization vector in the magnetic particle with respect to the flux line. Experiments with $Fe_2O_3 + MgB_2$ superconductor treated with high-intensity ultrasound without post sintering have confirmed the theory. A greater enhancement of magnetic hysteresis was observed for samples with embedded magnetic Fe_2O_3 nanoparticles than for non-magnetic Mo_2O_5 additions with a similar concentration and size distribution, figure 1(a), and the magnetically induced critical current density with Fe_2O_3 nanoparticle doping was consistently higher than for non-magnetic nanoparticles over the whole range of temperatures [15]. Data achieved for iron powder doped copper-clad PIT MgB_2 wires showed some improvement of the J_c. Further research will clarify whether a smaller level of Fe doping may improve pinning further and if sintering will not cause deterioration of the iron/MgB_2 interface. The dependence of the magnetic pinning force on the angle between the direction of magnetization in ferromagnetic nanoparticles and the flux lines may be of interest, and it is expected that oriented nanocomposite materials should have an anisotropic pinning enhancement [15, 19]. Importantly, as the contribution of the magnetic pinning force should be greater for materials with high Ginzburg–Landau coefficients, these results suggest a new direction in the improvement of magnetic vortex pinning in high-T_c superconductors [15].

Nanoparticulate Fe_3O_4 doping in polycrystalline MgB_2 has also been reported [20]. Strong fluctuations in the magnetization curves for low dopant concentrations reveal the occurrence of fluxoid jumps. A significant enhancement in J_c is, however, observed at low nano-Fe_3O_4 concentrations in the low temperature (20 K) and low magnetic field (<2 T)

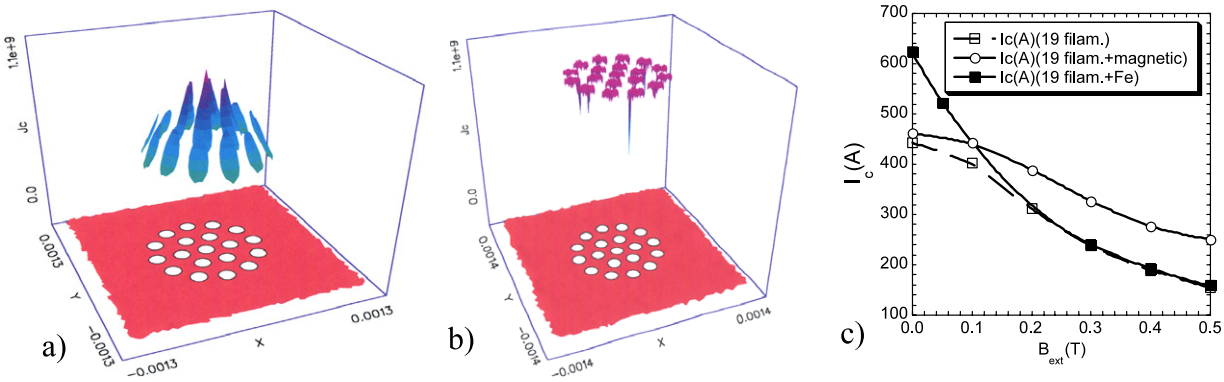

Figure 2. Spatial distribution of the critical current density in a 19-filament MgB_2 wire cross-section in self-field, for different values of relative magnetic permeability, μ_r, of concentric multi-screens: (a) $\mu_r = 1$, $I_c = 442$ A; (b) nonlinear Fe $\mu_{rmax} = 9000$, $I_c = 628$ A [1, 5]; (one may notice that the critical current density gradient across an individual filament can be as high as 20% of its nominal value. The gradient is different for the internal filaments, and the lowest J_c values are achieved for the external filaments); (c) transport critical current field dependences of the MgB_2 PIT filamentary conductors containing different superconducting–magnetic heterostructures.

regime [20]. These phenomena are attributed to the strong ferromagnetic nature of the iron oxide dopants dispersed in the MgB_2 matrix: vortices are depinned in the higher temperature and field regime. Mossbauer spectra showed that for higher doped concentrations, an extra intermetallic Fe–B, phase is probably produced in the sample, reducing the flux pinning [20]. The efficiency of ferromagnetic nanopinning centres has to be assessed on the basis of their size and chemical compatibility with MgB_2. It can be considered that the formation by low temperature processing of surface-passivated nanoparticles in ferromagnetically-doped *in situ* MgB_2 conductors is of prime importance for current research, even for the copper-clad *ex situ*/*in situ* MgB_2 composite conductor [21]. If the iron or Fe–O particle size decreases through the formation of Fe–B compounds at the Fe/MgB_2 interface, as has previously been reported [18], the surface/volume ratio would increase such that surface effects would strongly affect the magnetic properties. Therefore, in the absence of surface passivation, the contributory surface layer could greatly reduce the magnetic moment of the particle and cause reduction of the beneficial effect of the magnetic pinning effect.

In our experiments, iron powder of the diameter of 2 μm was added to the commercial 325 mesh powder of MgB_2 from Alfa Aesar, Johnson Matthew Company. Such a powder mixture was then ground in Planetary Micro Mill Pulverisette-7 made by FRITSCH GmbH. The actual conductors were prepared by compacting pure MgB_2 a mixture of MgB_2 (10 wt% Fe) and MgB_2 (25 wt% Fe) powders in a copper tubes OD = 6 mm ID = 5 mm and purity 99.99% using the powder-in-tube (PIT) method. After the final cold deformation steps of swaging and drawing, part of the doped and undoped and unreacted conductors were tested for magnetic critical current and the another parts of unreacted wires were sintered for 20 min at 850 °C under protective atmosphere of argon before magnetic measurements. Using a Quantum-Design SQUID magnetometer, magnetization versus magnetic field (M–H) curves of the round wires were measured at temperature of 6 K and magnetic fields up to 6 T to define the J_{cmag}. J_{cmag} was determined using the Bean critical state model for an infinitely long cylinder in parallel external magnetic field according to the formula $J_{cmag}(H) = 3/2[\Delta M(H)/R]$ where $\Delta M(H)$ is the width of the magnetization characteristic at applied magnetic field H and R is the radius of the cylinder. Distribution of the critical current in the multifilamentary conductor presented in figure 2 was conducted using electromagnetic software FLUXPD.

It was evident that the higher concentration of Fe in MgB_2 (25 wt% Fe) dominates the behaviour of the Cu/(MgB_2 + Fe) composite conductor irrespective of the sintering procedure, but data achieved for unreacted (10%Fe) doped copper-clad PIT MgB_2 (10 wt% Fe) wires showed 25% improvement of the J_{cmag} at 0.6 T in comparison to undoped conductor: see figure 1(b). After sintering of these conductors at 850 °C for 20 min Fe doped wire improved J_{cmag} up to 60%. Further research will clarify whether a smaller level of Fe doping and Fe nanoparticles may improve pinning further and if sintering under pressure of our new patented *in situ*/*ex situ* Fe doped conductors will cause deterioration of the Fe/MgB_2 interfaces. The dependence of the magnetic pinning force on the angle between the direction of magnetization in ferromagnetic nanoparticles and the flux lines may be of interest, and it is expected that oriented nanocomposite materials should have an anisotropic pinning enhancement [15, 19]. Importantly, as the contribution of the magnetic pinning force should be greater for materials with high Ginzburg–Landau coefficients, these results suggest a new direction in the improvement of magnetic vortex pinning in high-T_c superconductors [15].

3. MgB_2 multifilamentary conductors for ac applications with improved critical current

In multifilamentary MgB_2 conductors there are also important magnetic and cryogenic aspects of quench protection and stability. Firstly, to avoid flux jumps in large-filament MgB_2 conductors, use of a magnetic shielding material such as iron is advantageous to reduce large magnetic flux gradients in the superconducting filaments, see figure 2; and secondly, to

provide adequate cryogenic stabilization, an external highly conductive (thermally and electrically) metal is essential, such as copper [1].

Generally, AC losses in coated conductors are very sensitive to the magnetic field orientation relative to the conductor surface. Even for untextured MgB_2 coatings, the only way to effectively reduce losses is to align the filamentary conductors parallel to the external magnetic field. Increasing the number of filaments is very helpful in this case, but if the magnetic field can be correctly aligned along the conductor surface the losses will be minimal.

Since iron appears to be one of the favourable materials to be used as an 'inert' matrix especially for PIT conductors, we can explore the possibilities of superconducting–magnetic heterostructures [1] with the aim of minimizing ac losses for novel electrotechnical devices. Computer modelling was used to provide the foundation for the initial assessment of the optimum design for possible power applications. Generally, the ac losses in multifilamentary wires can be reduced by twisting filaments. The shorter the twist pitch length, the larger the ac loss reduction. The minimum practical twist pitch is approximately five times the diameter of the composite. While these twist pitches are fully effective in uniform external magnetic fields, they are only partially effective in non-uniform fields and are less effective with respect to the self-field of the composite. In self-field conditions, the twist does not change the self-field flux linked between the inner and outer filaments substantially and the current first fills the outer layers of the superconducting composite, similar to a solid superconductor. To decouple the filaments in self-field conditions, a magnetic screening method has been proposed [1, 13]. This method is extremely important for the coated conductor configuration and consists of surrounding each superconducting filament by a thin ferromagnetic layer. We have established by numerical modelling that magnetic shielding of the filaments reduces ac losses in self-field conditions due to decoupling of the filaments and, at the same time, it increases the critical current of the composite. Figure 2 shows an example of the critical current increase in the case of a shielded 19-filament composite. The critical current increased from about 440 A up to about 630 A in the magnetic self-field. This is due to the rather strong magnetic field dependence of the critical current density in the MgB_2 material.

4. $(BiPb)_2Sr_2Ca_2Cu_3O_9$ conductors

It was found experimentally that while most of the methods of decreasing the AC losses in $(BiPb)_2Sr_2Ca_2Cu_3O_9$ (Bi-2223) and $YBa_2Cu_3O_7$ tapes exposed to an external AC magnetic field [22–24] are successful, they are not effective in decreasing the transport AC losses, i.e. the self-field losses [26]. The self-field losses of $(BiPb)_2Sr_2Ca_2Cu_3O_9$ and $YBa_2Cu_3O_7$ tapes, regardless of whether they have a high resistivity matrix, oxide barriers around the filaments or twisted filaments, still scale with the theoretical relations for a monocore superconductor [24, 25]. This proves that in self-field conditions, the filaments in $(BiPb)_2Sr_2Ca_2Cu_3O_9$ and $YBa_2Cu_3O_7$ tapes are still magnetically coupled. The same is valid also for self-field losses in classical low-T_c superconductors [26]. To decouple the filaments, quite a large separation is needed, much larger than their dimensions [27–29]. Such a method would substantially decrease the current-carrying capacity of the composite. To decouple the filaments magnetically we propose instead to surround them with a suitable low-loss ferromagnetic material [13, 30, 31]. This method of magnetic decoupling can also be an effective technique to reduce the AC losses of multifilamentary superconductors exposed to moderate AC or DC external magnetic fields. In this paper we present results of numerical modelling of multifilamentary $(BiPb)_2Sr_2Ca_2Cu_3O_9$ tapes and $YBa_2Cu_3O_7$ coated conductors with filaments covered by a magnetic material such as soft iron with a nonlinear magnetization characteristic. All the calculations were performed in the fully-penetrated state in self-field using the critical state model with constant critical current density. The filaments were considered to have a rectangular cross-section because it has been found numerically that this geometry was more favourable from the point of view of the losses when the filaments were covered by magnetic layers [32]. There are also successful approaches to divert the magnetic flux in superconductors by introducing magnetic materials in proximity to the conductors [33, 34]. The magnetic cover method utilizes the shielding effect of magnetic material. In an idealized case, the magnetic field of a current-carrying filament embedded in a ferromagnetic material propagates outside and is screened by ferromagnetic coverings of the neighbouring filaments, so that the current distribution of the filaments inside these ferromagnetic coverings remains unaffected by the magnetic field of the current-carrying filament.

In figure 3 the role of magnetic screening of the Bi-2233 filaments in a model tape cross-section (not to scale) is presented. The conductor has 55 filaments, each of rectangular cross-section 250 μm $\times$ 30 μm, covered with a magnetic layer 5 μm thick. The separation between covered filaments is 20 μm in both directions. In figure 3(e) levels of the total loss in such a conductor are considered for coupled filaments, screened filaments and perfectly decoupled filaments.

5. Epitaxial surface oxidation (native oxide) of ferromagnetic substrates for $YBa_2Cu_3O_7$ coated conductors

Oxidation of highly-textured Ni-based ferromagnetic substrates is usually to be avoided as the oxide which grows is often of an unsuitable orientation or lattice match for deposition of buffer layers. However by controlling the conditions in which the substrate is oxidized it may be possible to produce an adherent epitaxial oxide with the cube texture. Any further buffer layers can then be deposited using an oxidizing environment, and substrate oxidation will not be a problem in the superconductor deposition stage. Indeed, if the oxide acts as a diffusion barrier, this may even remove the requirement for further buffer layers, in which case the surface oxidation epitaxy technique may serve as a fast and inexpensive buffer

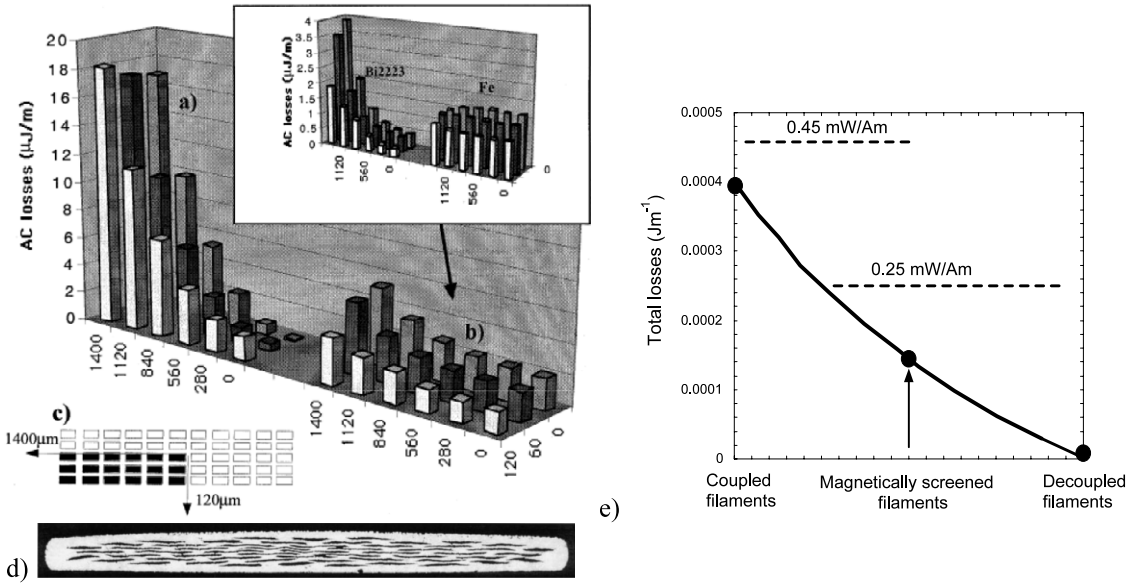

Figure 3. Contribution of the individual filaments in one quadrant of the 55-filamentary wire: (a) coupled filaments and (b) magnetically screened filaments (the inset shows the proportions of the loss in the superconducting material and the iron [22]); (c) the outline of the analysed quadrant in the model tape cross-section; (d) cross-section of the measured samples: 55 filaments, Ag–Mg external sheath and Ag matrix, dimensions of the tape: widths 3.65 mm, thickness 0.26 mm; (e) AC loss of 55-filament model conductor ($j_c = 1.16 \times 10^8$ A m^{-2}) with different degrees of interfilamentary coupling (from left): (1) coupled superconducting filaments (i.e., no magnetic cover present), (2) magnetically screened superconducting filaments (AC loss in superconducting filaments covered with iron layers $Q = 0.000\,07$ J m^{-1} plus the loss in the iron $Q = 0.000\,075$ J m^{-1}), (3) uncovered superconducting filaments with the iron but as if they were perfectly decoupled (i.e., mutually independent). The solid curve is a guide for the eye. The two horizontal lines represent two different goals (0.45 and 0.25 mW A^{-1} m^{-1}) for HTS to be competitive with copper wires.

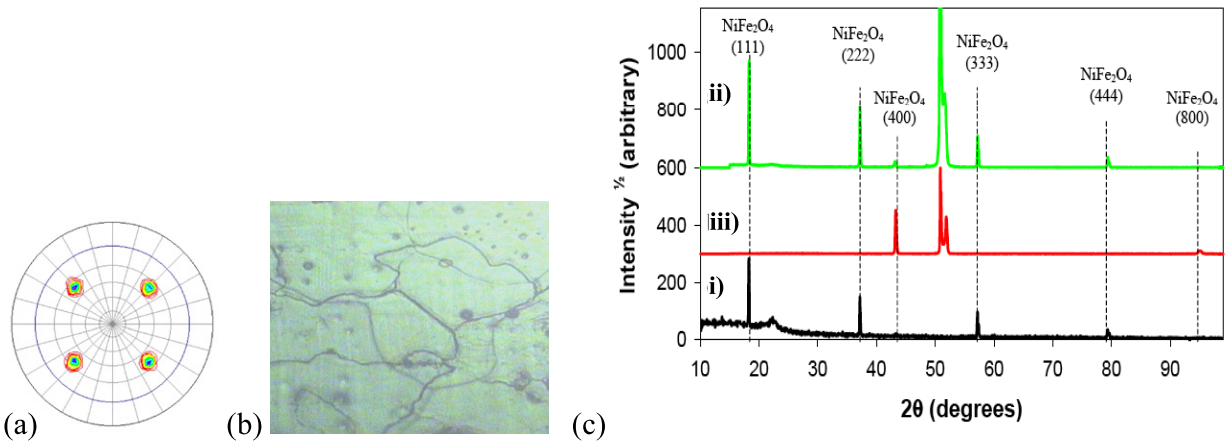

Figure 4. NiO layer on Ni substrates: (a) pole figure of the NiO; (b) optical image of the surface of a transparent SOE NiO/Ni grown at 1250 °C in air [35, 36]; (c) the (111) oxide (i) may be completely removed from the oxidized tape (ii) to leave behind a NiFe tape which has a cube-textured oxide layer (iii) [37, 38].

layer route. There have been successful attempts to use self-oxidation of Ni tapes [36–39], as presented in figure 4.

NiFe tapes have superior mechanical and structural properties to pure Ni substrates and some other Ni alloys. The oxidation process of NiFe tapes is more complicated due to the fact that mixed oxides may be formed; however, a two-stage spalling and re-oxidation process produces oxide which is (100) oriented [37]. The θ–2θ scans shown in figure 4(c) clearly show that the oxide that was removed had a (111) texture, whilst the remaining tape is covered with an oxide which is (100) oriented. The fact that a thin (100) layer remains on the surface may be utilized to consistently produce cube-textured oxides on the surface of the NiFe tape. It is likely that the oxide is neither entirely $NiFe_2O_4$ nor Fe_3O_4, but has some intermediate composition, best described as $(Ni_xFe_{1-x})^{2+}Fe_2^{3+}O_4$ [39].

This type of magnetic oxide buffer layer on a NiFe ferromagnetic substrate will require further development concerning scaling up the native oxide buffer layers to reduce the cost of the buffered coated conductor, and to prevent

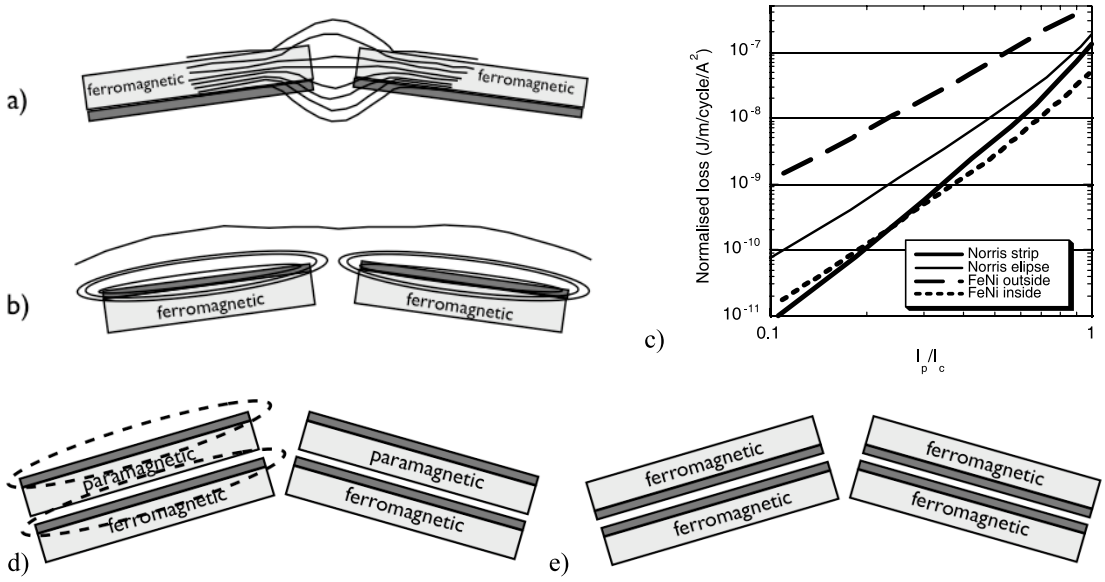

Figure 5. Possible cable architectures for $YBa_2Cu_3O_7$ deposited on a ferromagnetic substrate: (a) superconductor on the inner surface of the cable and (b) superconductor on the outer surface of the cable (in the picture, only a segment of the cable with two parallel tapes has been schematically presented). (c) AC transport losses for the two orientations of the coated conductor relative to the cable surface presented in (a) and (b), after [2]; (d) proposed new two-layer cable architecture in which the bottom layer is low cost; (e) proposed two-layer cable architecture in which both superconducting layers are low cost and facing each other, and the current is transmitted in the opposite direction.

extensive oxidation of the NiFe substrates and contamination of the $YBa_2Cu_3O_7$ coating. The magnetic properties of the native oxide layer may also be used in a novel deposition approach where coatings could be covered by magnetic material. The overall electron back-scattered diffraction, EBSD, maps of grain orientation, as well as data about misorientation from grain to grain, provides information about potential percolative current paths in the subsequent superconducting layer [40, 41].

6. Architecture of the coated conductors on ferromagnetic substrates in the coaxial cable configuration

The prospect of using low-cost, highly-textured Ni–Fe substrates [7] has stimulated research into potential superconducting cable architectures in which $YBa_2Cu_3O_7$ coated conductors with ferromagnetic substrates can be used [2, 42]. Modelling of two designs for a single-layer cable constructed from $YBa_2Cu_3O_7$ on a ferromagnetic substrate was presented by Miyagi *et al* [2], figures 5(a) and (b). It was proven that if the ferromagnetic substrate is on the inner surface of the cable, figure 5(b), the participation of the ferromagnetic material in AC losses can be negligible, whereas if the ferromagnetic material is on the outer surface of the cable the losses are substantially higher see figure 5(a). There are also possible solutions of new superconducting cable architectures presented in figures 5(d) and (e).

Similar calculations were conducted for two-layer cables by Sato *et al* [9] with special attention to the influence of the gap between the individual conductors. These calculations are valuable, but because they represent 2D models of a straight array of coated conductors along the cable they do not take into account the real helical configuration of the tapes in a multilayer superconducting cable [4, 43]. The influence of the transverse distribution of the current in a helical conductor has been taken into account by Majoros *et al* [3, 10–12], and this can clarify the mechanism responsible for the increased participation of the ferromagnetic substrate material in the overall losses of the cable. Calculations of the transport ac losses of the helix are presented by the authors in numerous publications that can be a correct analogue for the practical coated conductor cable under consideration.

While the radial magnetic field components are approximately the same on both surfaces, the axial field component B on the inner surface is nearly two times higher than that on the outer surface. From these results one can expect that the magnetic field start to penetrate into the tape from the inner surface of the helical solenoid. To estimate the ac losses at the edges of the tape one can then adopt the model of [44] and [45]. In this model it is supposed that the magnetic field is confined to one side of the superconducting sheet, which has a slit gap of width g parallel to the direction of the current flow [44, 45]. The sheet is supposed to be infinitely long, infinitely wide, with zero thickness and with constant critical current density, j, per unit width. As shown in [48], the correct expression for the loss, L_c, on both sides of the gap in a full cycle of the current is expressed by equation (1).

$$L_c = \frac{\mu_o j^2 g^2}{\pi}\left[2\ln\left|\cos\left(\frac{1}{2}\pi i\right)\right| + \frac{1}{2}\pi i \tan\left(\frac{1}{2}\pi i\right)\right]. \quad (1)$$

The main loss component comes from the axial magnetic field on the inner side of a helix (coming from the helicity). AC losses due to the gap between the tapes are only a small fraction of it. The only possibility of using coated conductors

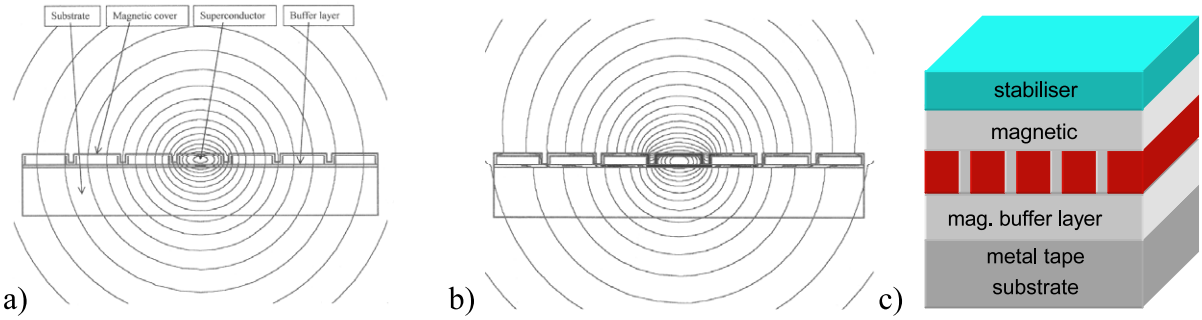

Figure 6. Magnetic field lines (scale 6×10^{-10} Wb) of a model coated conductor with 7 strips embedded in a ferromagnetic cover of rectangular cross-section, when the current with current density $j = 10^9$ A m^{-2} passes through the central filament only, after [31]: (a) $\mu_r = 1$ of all the materials (substrate, buffer layer and cover); (b) ferromagnetic cover $\mu_r = 1000$, substrate $\mu_r = 1$, ferromagnetic buffer layer $\mu_r = 1000$ (dimensions of the filaments: 8 μm $\times$ 2 μm, thickness of the ferromagnetic layer = 0.5 μm, spacing between the covered filaments = 1 μm, thickness of the buffer layer = 0.5 μm, thickness of the substrate = 9.5 μm), (c) schematic representation of a variety of straight multifilamentary coated conductor structures, with magnetic buffer and caps layer to provide magnetic decoupling and even electric decoupling of the filaments [48].

with ferromagnetic substrates is in a 2-layer coaxial cable in which the outer layer serves as a return conductor. In the ideal case, with a small inter-layer separation, there is no magnetic field inside or outside of it: the magnetic field exists only in the space between the two layers. So we can imagine the use of a coated conductor tape with a ferromagnetic substrate inside (in the inner layer) and outside (in the outer layer) of the cable so that the substrates could not see any magnetic field. The minimum layer separation is determined by the thickness of the insulation, which depends on the voltage level used [46]. This cable architecture was originally developed in Brookhaven National Laboratories some decades ago using Nb_3Sn tapes, see e.g. [46].

7. Multifilamentary YBCO coated conductors for AC applications

Because (RE)$Ba_2Cu_3O_7$ coated conductors are characterized by a high irreversibility line and high J_c values in external magnetic fields, they are among the most promising candidates for power applications such as generators or motors [47]. Advances in multifilamentary $YBa_2Cu_3O_7$ coated conductor technology such as laser grooving, ink jet patterning and ink jet printing may allow the manufacture of narrow filaments with high critical current density on a thin non-magnetic metal alloy substrate which is separated from the superconductor by a thin dielectric, conductive or even magnetic buffer: see figure 6(c).

There are many issues that should be addressed during the design stage of a coated conductor for AC transport current and AC external field applications before actual optimization of the deposition processes of the conductor takes place. The transverse resistivity across the filamentary structure depends: on the resistivity of $YBa_2Cu_3O_7$/metal layer boundary, which affects the current transfer length, on the resistance of the metal layer covering the filaments per unit length, and finally on the width and J_c of $YBa_2Cu_3O_7$ filaments. In the case of filaments with highly conductive stabilizers only on top of the filaments, the transverse resistivity between filaments can be high.

7.1. Decrease of transport ac losses in multifilamentary superconductors by ferromagnetic coatings

It is clear from the simulation presented in figure 6 that only in the case of both a ferromagnetic buffer layer and a ferromagnetic cover will the flux generated by the central filament be diverted away from the neighbouring filaments, figure 6(b).

The experimental data for transport ac losses in multifilamentary wires and tapes (both low-T_c and high-T_c) lie between two theoretical limits for a monocore superconductor of circular or elliptical cross-section and a thin strip, derived from the critical state model. According to this model [47] the transport ac losses Q with a transport current of amplitude I_o for a monocore superconductor are, for an elliptical or circular cross-section equation (2):

$$Q = \frac{\mu_o I_c^2}{\pi}\left[(1-i)\ln(1-i) + (2-i)\frac{i}{2}\right] \qquad (2)$$

and for a thin strip superconductor equation (3)

$$Q = \frac{\mu_o I_c^2}{\pi}\left[(1-i)\ln(1-i) + (1+i)\ln(1+i) - i^2\right] \qquad (3)$$

where Q is the loss energy per cycle in joule per unit length of the superconductor, I_c is the critical current of the monocore superconductor and the parameter $i = I_o/I_c$ is the normalized current.

The theoretical losses, equations (2) and (3), are hysteretic losses and they do not depend on frequency. From these relations it is seen that the transport ac losses for a monocore superconductor with either circular, elliptical or thin strip cross-section can be written as equation (4)

$$Q_{mono} = a I_c^2 F(i) \qquad (4)$$

where $a = \mu_o/\pi$ and $F(i)$ is a functional dependence characterizing the geometrical form of the cross-section. In the case of N identical and independent (i.e. magnetically decoupled) filaments, the same theoretical equation (4) holds

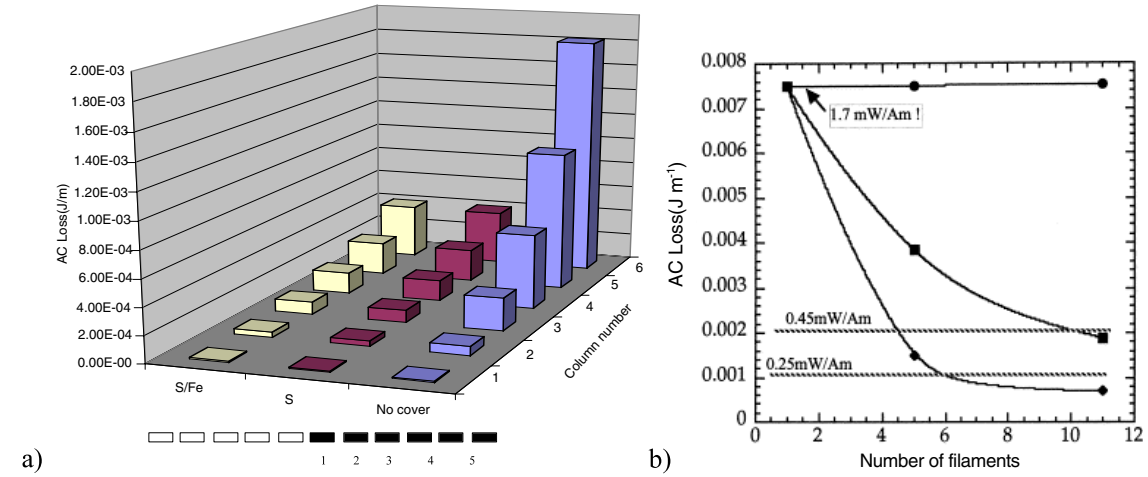

Figure 7. (a) AC loss distribution in individual filaments when they are covered with Fe layers and without the covering. (S/Fe—total losses, S—part of the losses only in the superconductor). Only the filaments from the cross-section marked in black are shown; (b) AC loss in superconducting material of a model coated conductor ($j_c = 10^{10}$ A m^{-2}) as a function of the number of filaments (constant amount of superconducting material, iron layer thickness 1 μm, separation between covered filaments 5 μm). (●—coupled filaments, i.e. no magnetic cover, ■—magnetically screened filaments, ♦—decoupled filaments, i.e. no magnetic cover but the filaments mutually independent). The curves are a guide for the eye, and the horizontal lines represent two different goals (0.45 and 0.25 mW A^{-1} m^{-1}) for HTS to be competitive with copper wires [22].

for each filament, but this time I_c is the critical current of a single filament which we denote I_{c1} [31]. Transport ac losses of such a multifilamentary superconductor Q_{multi} are then the sum of the losses of each individual filament Q_1, i.e. $Q_{multi} = NQ_1$. Similarly the critical current of such a multifilamentary superconductor is simply the critical current of the individual filament I_{c1} multiplied by the number of filaments, i.e. $I_{cmulti} = NI_{c1}$, and the parameter i is the same for the monocore and multifilamentary superconductors, because $i_{mono} = I_o/I_c = NI_{o1}/(NI_{c1}) = i_{multi}$. Hence the ratio K of the losses in a monocore superconductor Q_{mono} to the losses in a multifilamentary superconductor with magnetically decoupled filaments Q_{multi} is equation (5):

$$K = \frac{Q_{mono}}{Q_{multi}} = \frac{aI_c^2F(i)}{aNI_{c1}^2F(i)} = \frac{I_c^2}{NI_{c1}^2} = \frac{(NI_{c1})^2}{NI_{c1}^2} = N. \quad (5)$$

From this analysis it is clear that magnetic decoupling of the filaments significantly decreases the transport ac losses, proportionally to the number of filaments N, which in the case of e.g. 100 filaments means an overall decrease in the losses by two orders of magnitude [31].

To decouple the filaments magnetically we propose to surround them by a suitable ferromagnetic material. From a theoretical analysis of a single filament surrounded by ferromagnetic material [32], it follows that while for a superconductor with circular cross-section the presence of a magnetic coating does not influence the magnetic field distribution within the superconductor or the transport ac losses, for a superconductor with an elliptical cross-section, the magnetic coating affects both the magnetic field distribution and the transport ac losses. The same is also expected to be valid for I_c.

When estimating the overall transport ac loss decrease by magnetic decoupling of the filaments, equation (5) must be modified by taking into account the ac loss increase in the superconductor itself by the presence of the magnetic coating, its I_c degradation and the hysteretic losses in the magnetic coating as well. Because the theoretical results are unknown, we introduced an additional parameter k that contains the effect of the ac loss increase in both materials, the superconductor and the magnetic coating [31]. The critical current of a coated single filament is $I_{c1coated} = \alpha I_{c1}$ where the parameter α characterizes the I_c degradation by the coating. Then the ac losses of a single coated filament can be expressed by equation (6):

$$Q_{1coated} = kaI_{c1coated}^2F(i) = ka\alpha^2I_{c1}^2F(i). \quad (6)$$

Then ac losses in the multifilamentary superconductor with magnetically coated filaments can be defined by equation (7):

$$Q_{multicoated} = NQ_{1coated} = Nka\alpha^2I_{c1}^2F(i). \quad (7)$$

In comparison with a monocore superconductor at the same reduced current i one obtains in the form of equation (8):

$$K'' = \frac{Q_{mono}}{Q_{multicoated}} = \frac{aI_c^2F(i)}{Nka\alpha^2I_{c1}^2F(i)} = \frac{N^2I_{c1}^2}{Nk\alpha^2I_{c1}^2} = \frac{N}{k\alpha^2} \quad (8)$$

where the parameters, k and, α, are to be determined from experiment. Example results of the ac losses calculation for an 11-filament coated conductor covered by ferromagnetic material are presented in figure 8.

The beneficial influence of the magnetic decoupling of individual filaments in the coated conductor by ferromagnetic material is clearly presented in figure 7.

If instead of the non-magnetic substrate, a ferromagnetic NiFe substrate is also used, the magnetic flux along the YBCO c-axis will be amplified. To divert the flux a ferromagnetic buffer layer and ferromagnetic coating will be needed as presented in figure 8(b).

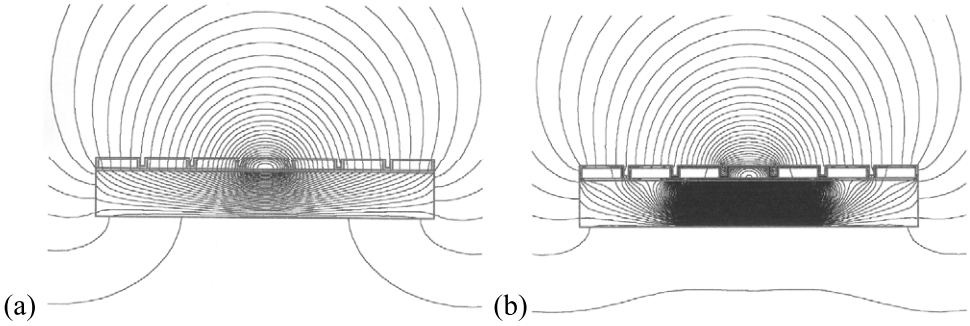

Figure 8. Magnetic field lines (scale 6×10^{-10} Wb) of a model coated conductor with 7 strips embedded in a ferromagnetic cover of rectangular cross-section, when a current with current density $j = 10^9$ A m^{-2} passes through the central filament only: (a) $\mu_r = 1$ of the buffer layer and cover materials where substrate $\mu_r = 1000$, (b) $\mu_r = 1000$ for all the materials (substrate, buffer layer and cover).

8. Conclusion

In this paper we have provided evidence that the proximity of ferromagnetic materials may benefit the performance of superconducting conductors in respect of the critical current and ac losses. These very encouraging results will be further explored to bring a better understanding of the role of magnetic coatings and magnetically enhanced pinning in doped superconductors including MgB_2 and HTS.

The presence of ferromagnetic materials may influence the performance of superconductors on the nano, micro and macroscales. Despite the evidence that ferromagnetic materials in proximity to the superconducting material can substantially improve superconducting parameters, there is a need for further research to determine the behaviour of ferromagnetic pinning centres subjected to high temperature sintering conditions, during which the interface between the superconductor and ferromagnet can be strongly modified by interdiffusion processes. Also it is important to define the optimum size and shape for pinning centres: it is not yet obvious if the magnetic inclusions should be single-domain or multi-domain particles to achieve the optimum magnetic flux interaction.

There is also a necessity to develop thicker epitaxial native oxide layers on ferromagnetic NiFe substrates that would provide low-cost buffered RABiTS for the high performance coated conductor. It is envisaged that ink jet printing is one of the most promising techniques to provide fully-assembled, multilayer, multifilamentary coated conductors including YBaCuO, screening magnetic coatings and silver-based conductive stabilization layers. Such low-cost coated conductors could be applied in AC applications including the composite superconducting cables discussed here and also NMR electromagnets, in which the proximity of ferromagnetic substrates would not be detrimental to coated conductor performance.

References

[1] Glowacki B A, Majoros M, Vicker M, Eisterer M, Toenies S, Weber H W, Fukutomi M, Komori K and Togano K 2003 *Supercond. Sci. Technol.* **16** 297
[2] Miyagi D, Umabuchi M, Takahashi N and Tsukamoto O 2007 *Physica* C **463–465** 785–9
[3] Majoros M, Glowacki B A, Campbell A M, Han Z and Vase P 1999 *Physica* C **314** 1
[4] http://www.msm.cam.ac.uk/ascg/lectures/applications/cables.php
[5] Glowacki B A and Majoros M 2001 *Studies of HTS Superconductors (Advances in Research and Applications) MgB_2* vol 38, ed A Narlikar (Huntington, NY: Nova Science) pp 361–96
[6] Al-Mosawi M K, Beduz C, Goddard K, Sykulski J K, Yang Y, Xu B, Ship K S, Stoll R and Stephen N G 2002 *Physica* C **372–376** 1539
[7] Glowacki B A, Vickers M, Rutter N, Maher E, Pasotti F, Baldini A and Major R 2002 *J. Mater. Sci.* **37** 157
[8] Denul J, Van Drissche I, te Lintelo H, De Gryse R, Tsetsekou A, Hoste S, Glowacki B A, Garre R, Maher E, Good J, Ranucci E and Larrauri E 2000 *Inst. Phys. Conf. Ser.* **167** 335
[9] Sato S and Amemiya N 2006 *IEEE Trans. Appl. Supercond.* **16** 127
[10] Majoros M, Glowacki B A, Campbell A M, Han Z and Vase P 2000 *Inst. Phys. Conf. Ser.* **167** 839
[11] Majoros M, Glowacki B A, Campbell A M, Han Z and Vase P 1998 *Physics* C **310** 95
[12] Majoros M and Glowacki B A 2000 *Studies of HTS Superconductors (Advances in Research and Applications): AC Losses and Flux Pinning and Formation of Stripe Phase* vol 32, ed A Narlikar (Huntington, NY: Nova Science) pp 1–51
[13] Glowacki B A and Majoros M 2000 *Supercond. Sci. Technol.* **13** 483
[14] http://msm.cam.ac.uk/ascg/lectures/electronics/superferro.php
[15] Snezhko A, Prozorov T and Prozorov R 2005 *Phys. Rev.* B **71** 024527
[16] Prozorov T, Prozorov R, Snezhko A and Suslick K S 2003 *Appl. Phys. Lett.* **83** 2019
[17] Singh K P, Awana V P S, Balamurugan S, Shahabuddin M, Singh H K, Husain M, Kishan H, Bauminger E R and Felner I 2008 *J. Supercond.* **21** 39
[18] Grovenor C R M, Goodsir L, Salter C J, Kovac P and Husek I 2004 *Supercond. Sci. Technol.* **17** 479
[19] Prozorov R, Prozorov T and Snezhko A 2005 *IEEE Trans. Appl. Supercond.* **15** 3277
[20] Singh K P, Awana V P S, Balamurugan S, Shahabuddin M, Singh H K, Husain M, Kishan H, Bauminger E R and Felner I 2008 *J. Supercond. Novel Magn.* **21** 39
[21] Glowacki B A and Nuttall W J 2008 *J. Phys.: Conf. Ser. (EUCAS'07)* **97** 012333

[22] Glowacki B A, Majoros M, Rutter N R and Campbell A M 2001 *Cryogenics* **41** 103
[23] Kwasnitza K, Clerk St, Flukiger R, Huang Y B and Grasso G 1997 *Inst. Phys. Conf. Ser. No 158 (Appl. Supercond.)* **2** 1389
[24] Huang Y B *et al* 1998 *J. Supercond.* **11** 495
[25] Eckelmann H, Dumling M, Quilitz M and Goldacker W 1998 *Physica* C **295** 198
[26] Salmon D E and Catterall J A 1970 *J. Phys. D: Appl. Phys.* **3** 1023
[27] Hughes T J, Yang Y and Beduz C 1999 *IEEE Trans. Appl. Supercond.* **9** 774
[28] Hughes T J, Yang Y, Beduz C and Power A 1998 *Physica* C **310** 187
[29] Müller K H 1997 *Physica* C **289** 123
[30] Glowacki B A and Majoros M 2000 *Supercond. Sci. Technol.* **13** 971
[31] Majoros M, Glowacki B A and Campbell A M 2000 *Physica* C **334** 129
[32] Majoros M, Glowacki B A and Campbell A M 2001 *IEEE Trans. Appl. Supercond.* **11** 2780
[33] Gomory F, Souc J, Seiler E, Vojenciak M and Granados X 2008 *J. Phys.: Conf. Ser.* **97** 012096
[34] Gomory F, Vojenciak M, Souc J and Seiler E 2008 *Acta Phys. Pol.* A **113** 605
[35] Kursumovic A, Huhne R, Tomov R, Glowacki B A, Evetts J E and Holzapfel B 2003 *Acta Mater.* **51** 3759
[36] Kursumowic A, Tomov R, Glowacki B A, Evetts J E, Tuissi A, Villa E and Holzapfel B 2003 *Physica* C **385** 337
[37] Rutter N A 2001 Microstructural development and superconducting parameters of the $YBa_2Cu_3O_{7-\delta}$ coated conductor (supervisor Glowacki B A) *PhD Thesis* Department of Materials Science and Metallurgy, University of Cambridge, Cambridge
[38] Rutter N A, Glowacki B A, Durrell J H, Evetts J E, te Lintelo H, De Gryse R and Denull J 2000 *Inst. Phys. Conf. Ser.,* **167** 407
[39] Putnis A 1992 *An Introduction to Mineral Sciences* (Cambridge: Cambridge University Press)
[40] Rutter N A and Glowacki B A 2001 *IEEE Trans. Appl. Supercond.* **11** 2730
[41] Zaimetz B, Glowacki B A and Evetts J E 2002 *Eur. Phys. J.* B **29** 359
[42] Suenaga M, Iwakuma M, Sueyoshi T, Izumi T, Mimura M, Takahashi Y and Aoki Y 2008 *J. Phys.: Conf. Ser.* **97** 012025
[43] Glowacki B A 2006 *Adv. Sci. Technol.* **47** 246
[44] Norris W T 1970 *J. Phys. D: Appl. Phys.* **3** 489
[45] Majoros M 1996 *Physica* C **272** 62
[46] Forsyth E B and Thomas R A 1986 *Cryogenics* **26** 599
[47] Oberly C E, Long L, Rhoads G L and Carr W J Jr 2001 *Cryogenics* **41** 117
[48] Glowacki B A 2005 *Frontiers in Superconducting Materials* ed A Narlikar (Berlin: Springer) p 765